Sun et al. Supplemental Figure S1

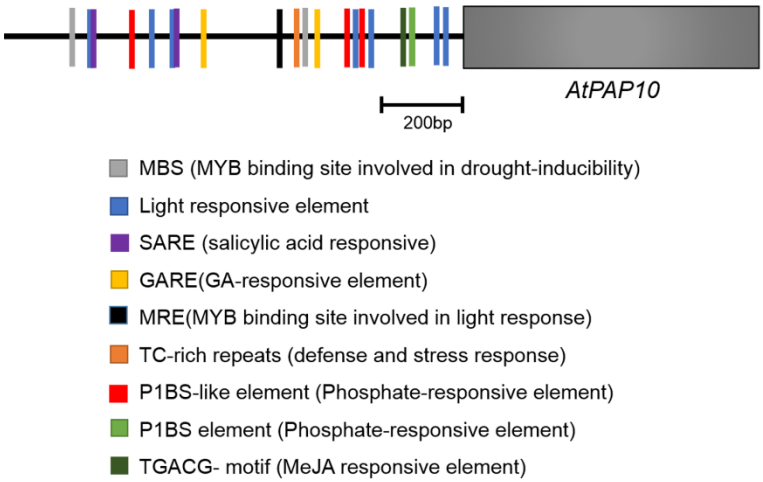

Supplemental Figure S1. A diagram showing the various *cis*-elements in a 1.0-kb sequence upstream of the start codon of the *AtPAP10* gene.

Sun et al. Supplemental Figure S2

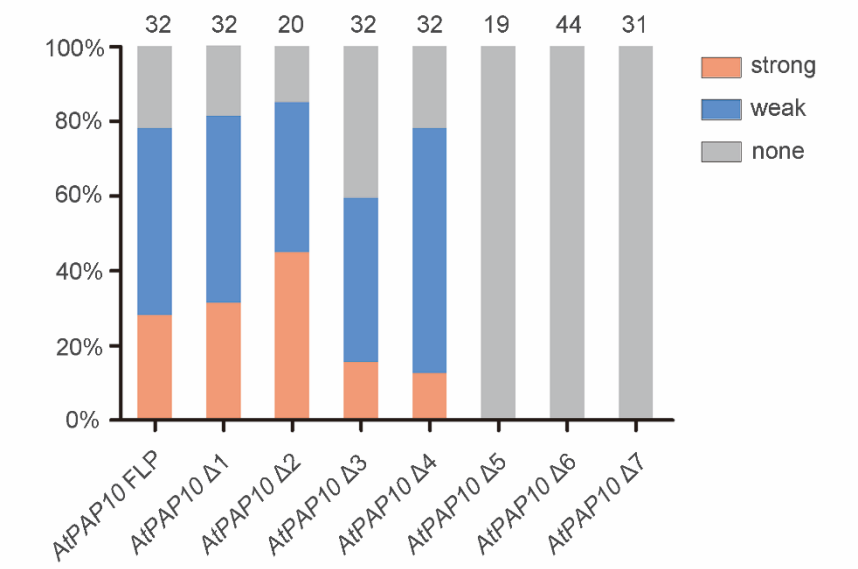

Supplemental Figure S2. Summary of the GUS activity for the transgenic plants carrying various deletion constructs of the *AtPAP10* promoter. The name of each construct is shown at the bottom. The number of independent transgenic lines obtained for each construct is indicated on the top. GUS staining activities for these transgenic lines were visually rated as “strong”, “weak”, and “none”.

Sun et al. Supplemental Figure S3

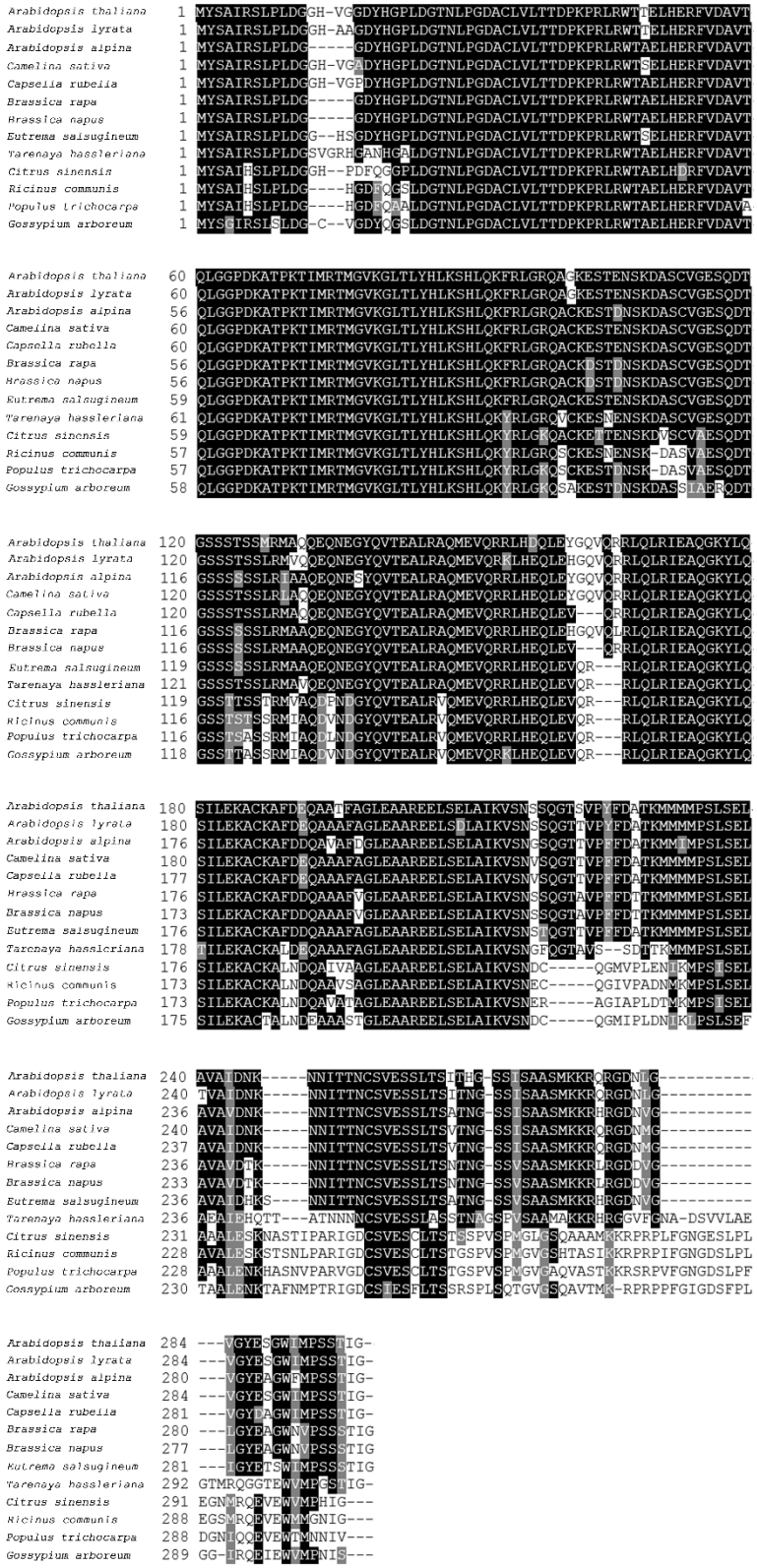

Supplemental Figure S3. Alignment of protein sequences of PHL2 and its orthologs in other plant species. The names of the plant species are indicated at the left. The alignment was generated using the Clustal W2 program. Identical and similar amino acids among the different plant species are highlighted with black and grey background, respectively. Numbers at the left indicate the positions of amino acid residues.

Sun et al. Supplemental Figure S4

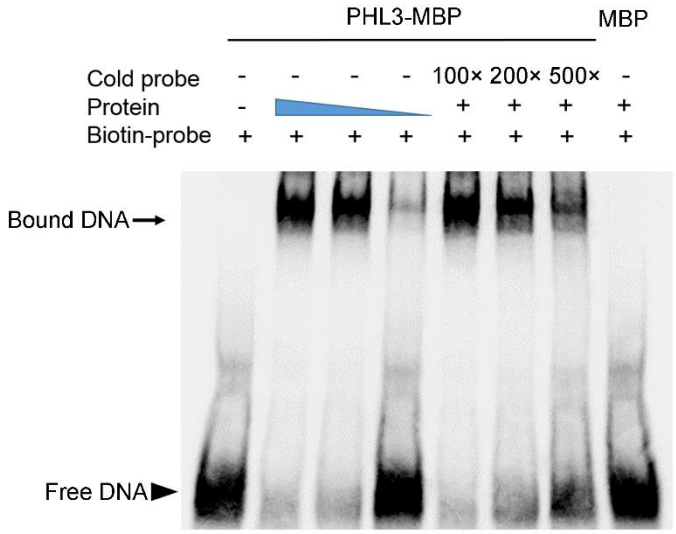

Supplemental Figure S4. EMSA assays showing the binding of recombinant PHL2-MBP fusion protein to the P sequence. The experiment was performed using 0.1, 0.05, and 0.01 μg of PHL3-MBP proteins. The unlabeled probe of the P sequence was used as a competitor DNA at an excess molar ratio of 100:1, 200:1, and 500:1 to the labeled probe.

Sun et al. Supplemental Figure S5

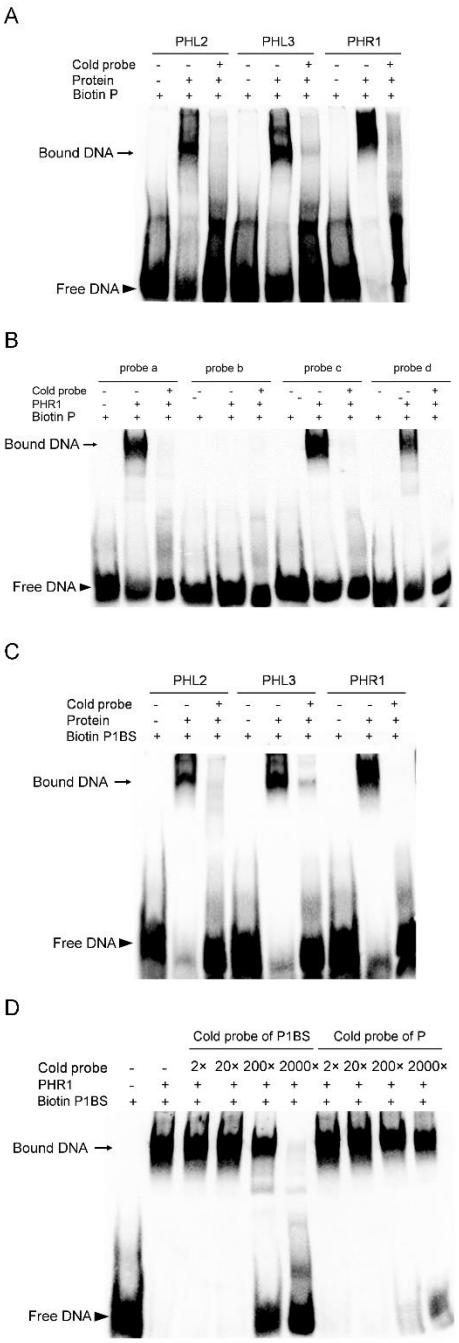

Supplemental Figure S5. EMSA assays showing the binding of PHL2 and PHL3 to the P1BS element and the binding of PHR1 to the P sequence. A, EMSA assay showing the binding of PHL2, PHL3, and PHR1 to the P sequence. B, EMSA assays showing the binding of PHR1 to the different parts of the P sequence (for the relative position of these different parts within the P sequence, see Figure 4A). C, EMSA assay showing the binding of PHL2, PHL3, and PHR1 to the P1BS element. D, EMSA assay showing the relative binding affinity of PHR1 to the P1BS element and the P sequence. PHR1 was first incubated with biotin-labelled P1BS element. The unlabeled probes of P1BS or P sequence at an excess molar ratio of 2:1, 20:1, 200:1, and 2000:1 were then added to the reaction mixture before electrophoresis. In (A), (B), and (C), the unlabeled probe of the P sequence or of the P1BS element was used at an excess molar ratio of 500:1. For all experiments, 0.05 μg recombinant proteins were used.

Sun et al. Supplemental Figure S6

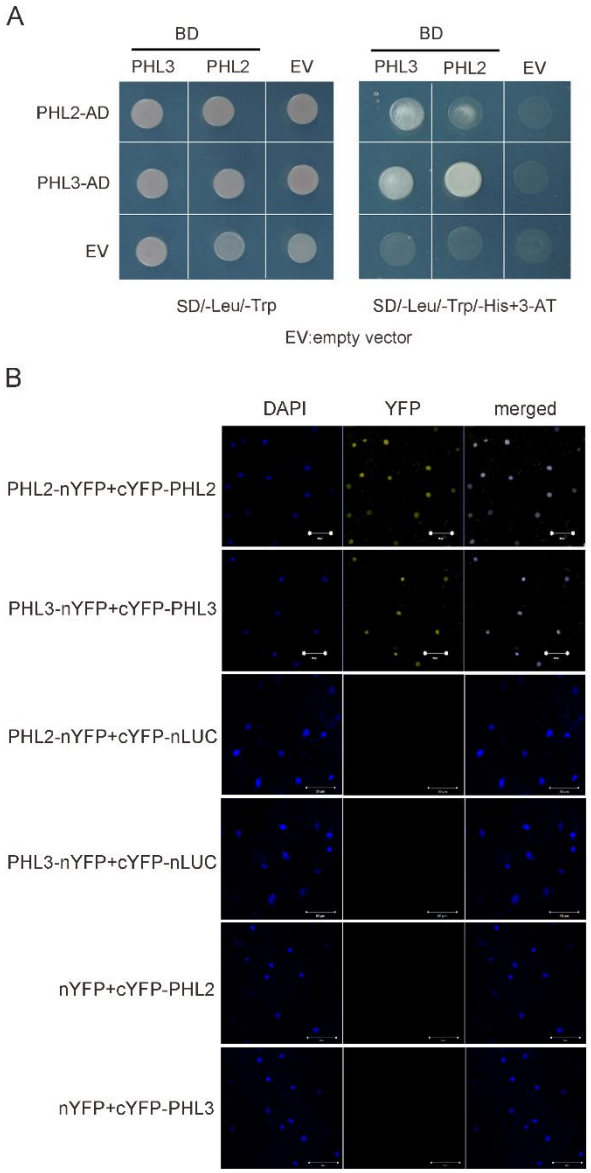

Supplemental Figure S6. Interactions between PHL2 and PHL3 and with themselves. A, Yeast two-hybrid assays showing the interaction between PHL2 and PHL3 and with themselves. Both PHL2 and PHL3 were fused with the GAL4 DNA-binding domain (BD) or the activation domain (AD). Yeast cells co-transformed with different combinations of PHL2 and PHL3 expression vectors were grown on control (SD/-Leu/Trp) and selective (SD/-Leu/Trp/-His+2.5 mM 3-AT) media. EV: empty vector. B, BiFC assays showing the self-interactions of PHL2 and PHL3. YFP signals were observed in the leaves of *N. benthamiana* co-expressing *PHL2-nYFP* and *cYFP-PHL2* or *PHL3-nYFP* and *cYFP-PHL3* driven by the 35S promoter. No signal of YFP was detected in plants co-expression constructs *PHL2-nYFP*/*cYFP-nLUC*, *PHL3-nYFP*/*cYFP-nLUC*, *nYFP*/*cYFP-PHL*2, or *nYFP*/*cYFP-PHL3.* The location of the nuclei is indicated by DAPI staining.

Sun et al. Supplemental Figure S7

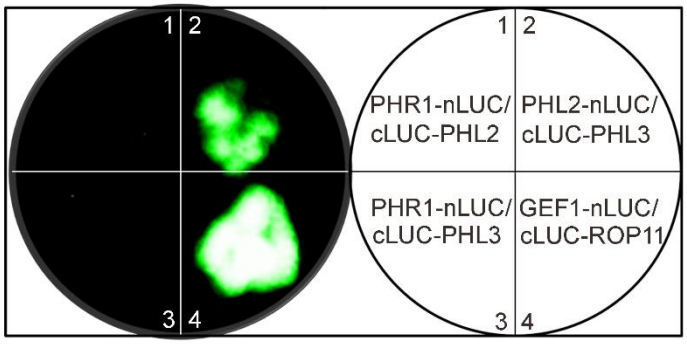

Supplemental Figure S7. LCI assays showing the absence of interaction between PHR1 and PHL2 or PHL3. The construct *PHR1-nLUC* was co-transformed with *cLUC-PHL2* or *cLUC-PHL3* into the leaves of *N. benthamiana*. As a positive control, the constructs *PHL2-nLUC*/*cLUC-PHL3* or *GEF1-nLUC*/*cLUC-ROP11* (Li et al., 2012) were co-transformed into the leaves of *N. benthamiana*. LUC activity was observed two days after *Agrobacterium* infiltration.

Sun et al. Supplemental Figure S8

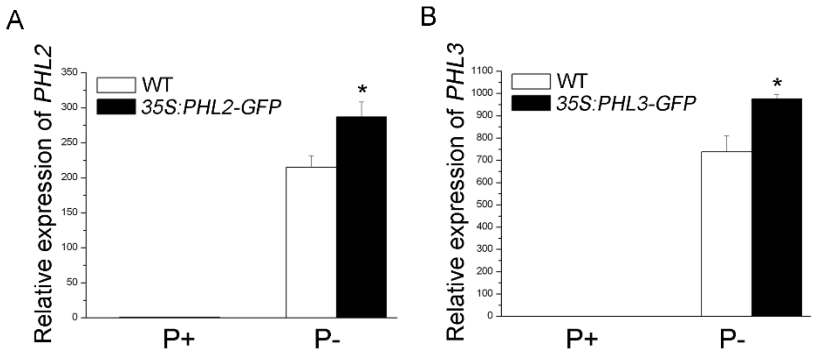

Supplemental Figure S8. The relative expression of *GFP-PHL2* and *GFP-PHL3* under P+ and P- conditions. Total RNAs were extracted from 8-day-old seedlings of the WT and transgenic lines carrying the *35S:GFP-PHL2* or *35S:GFP-PHL3* construct. The expression levels of *GFP-PHL2* and *GFP-PHL3* were determined by qPCR analysis. Values are means ± SE of three replicates. Asterisks indicate a significant difference from the WT under same growth conditions (Student's *t*-test, $P<0.05$).

Sun et al. Supplemental Figure S9

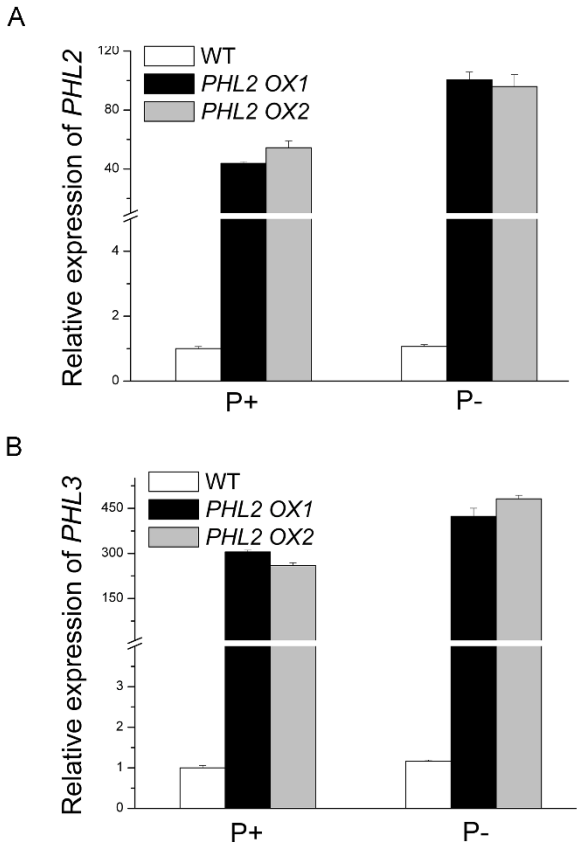

Supplemental Figure S9. The relative expression of *PHL2* and *PHL3* genes in *PHL2*- and *PHL3*-overexpressing lines. Total RNAs were extracted from 8-day-old seedlings of the WT and two independent transgenic lines carrying the *35S:PHL2* or *35S:PHL3* construct. The expression levels of *PHL2* and *PHL3* were determined by qPCR. Values are means ± SE of three replicates. Asterisks indicate a significant difference from the WT under same growth conditions (Student's *t*-test, $P<0.05$).

Sun et al. Supplemental Figure S10

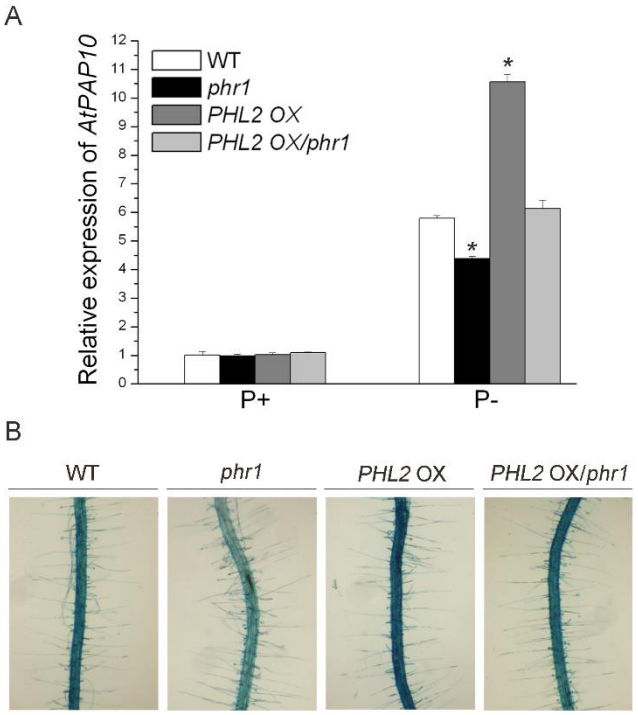

Supplemental Figure S10. Relative expression of *AtPAP10* and root-associated APase activity in *phr1* plants overexpressing *PHL2* (*PHL2 OX/phr1*). *PHL2 OX* was crossed with *phr1*. Plants overexpressing *PHL2* in the *phr1* background were selected in the F_2 population. (A) and (B) show relative expression of *AtPAP10* and BCIP staining of root-associated APase activity, respectively, in 8-day-old WT, *phr1*, *PHL2 OX*, and *PHL2 OX*/*phr1* seedlings .

Sun et al. Supplemental Figure S11

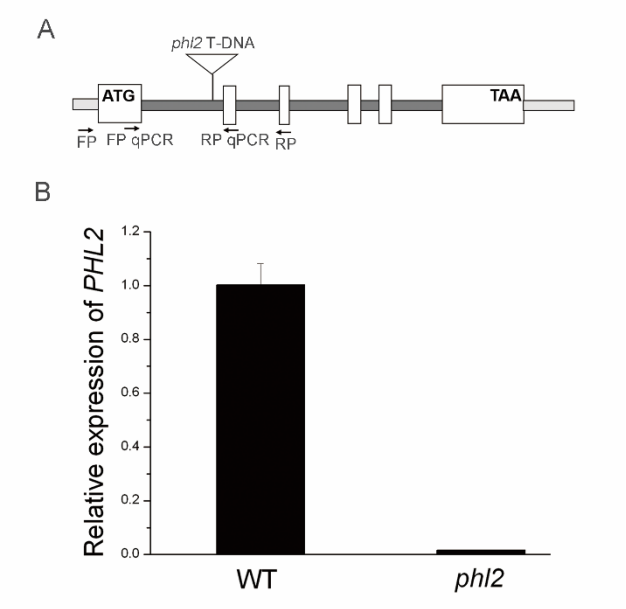

Supplemental Figure S11. Identification of the *phl2* knockout mutant. A, Schematic diagram showing the position of the T-DNA insertion sites in the *PHL2* gene of the SALK_114420C line. White box: exon; dark gray rectangle: intron; light gray rectangle: UTR; white triangle: T-DNA insertion site. FP and RP are primer pairs for identification of T-DNA insertion. FP qPCR and RP qPCR are primer pairs for qPCR analysis. B, Relative expression of *PHL2* in 8-day-old WT and SALK_114420C seedlings. Values are means ± SE of three replicates.

Sun et al. Supplemental Figure S12

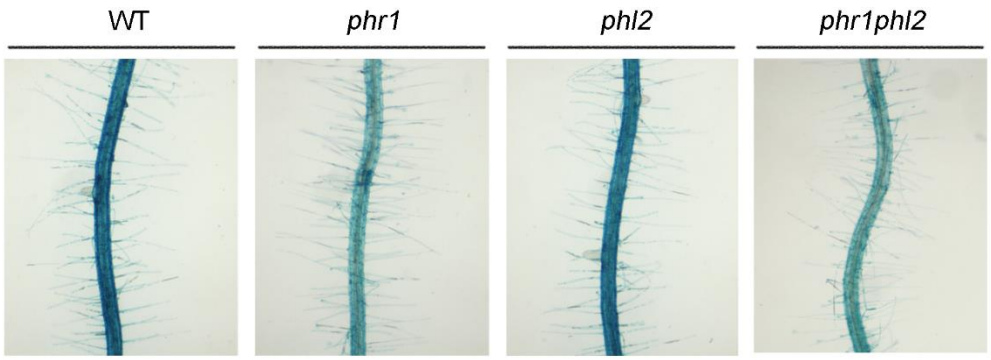

Supplemental Figure S12. BCIP staining of root-associated APase activity in 8-day-old WT, *phr1*, *phl2* and *phr1phl2* seedlings grown under P- condition.

Sun et al. Supplemental Figure S13

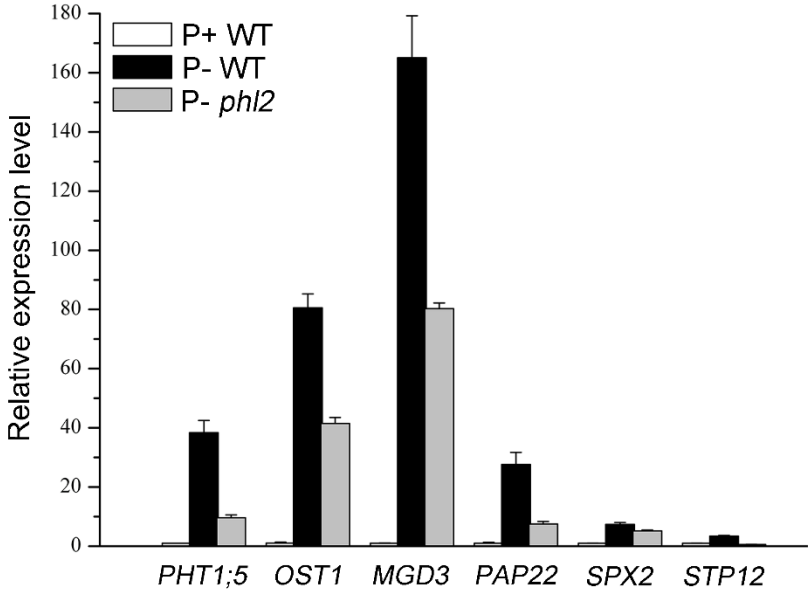

Supplemental Figure S13. Validation of the RNA-seq results by qPCR analysis. The relative expression of six PSI genes selected from RNA-seq analysis was analyzed by qPCR. Total RNAs were extracted from the roots of 8-day-old WT seedlings grown under both P+ and P- condition and from *phl2* seedlings grown under P- condition. Values are means ± SE of three replicates. The names of the genes examined are indicated at the bottom.

Sun et al. Supplemental Figure S14

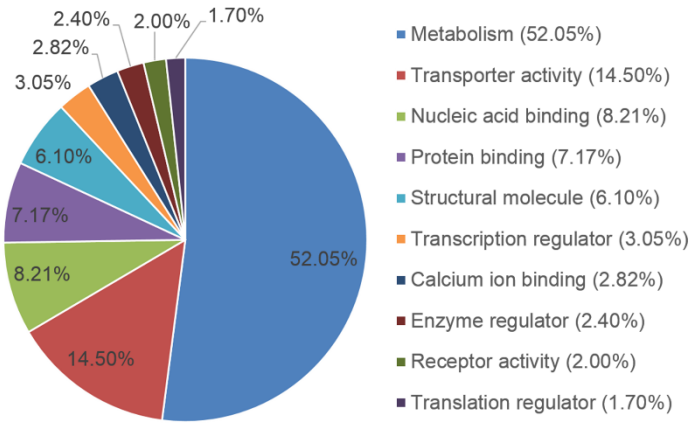

Supplemental Figure S14. GO analysis of PSI genes whose expression was significantly reduced in *phl2* (lower than 70% of that in P- WT).

Sun et al. Supplemental Figure S15

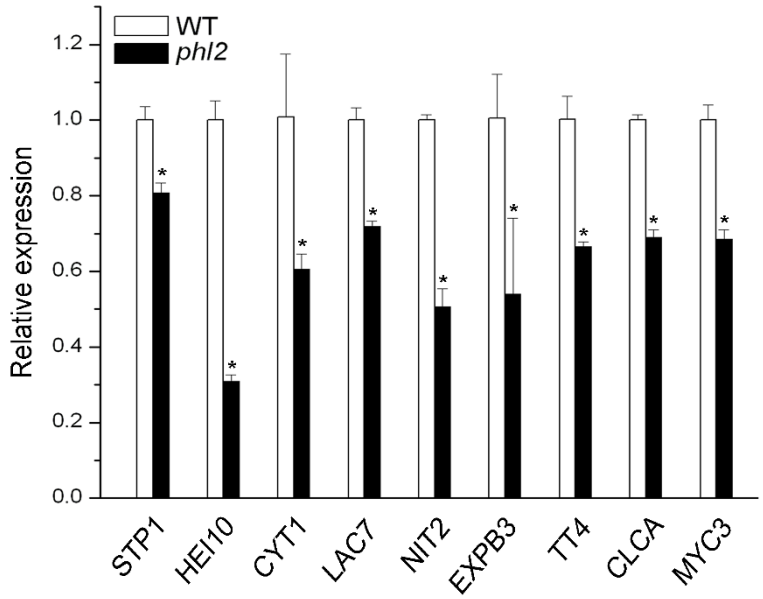

Supplemental Figure S15. Expression analysis of nine non-PSI genes under normal growth condition. The relative expression of nine non-PSI genes selected from RNA-seq analysis was analyzed by qPCR analysis. Total RNAs were extracted from the roots of 8-day-old WT and *phl2* seedlings grown under P+ condition. Values are means ± SE of three replicates. The names of the genes examined are indicated at the bottom.